

Tritium recovery in ITER by radiative plasma terminations

D.G. Whyte^{a,*}, J.W. Davis^b

^a University of Wisconsin – Madison, 331 Engineering Research Building, 1500 Engineering Dr. Madison, WI 53706, USA

^b University of Toronto, Institute for Aerospace Studies, Toronto, ON Canada M3H 5T6

Abstract

Planned radiative plasma terminations are examined as a method to recover tritium from plasma-deposited layers in the ITER tokamak. The technique exploits the high energy density of the ITER plasma, which is converted into a quasi-uniform radiation pulse by massive impurity injection that benignly terminates the plasma discharge. The radiation pulse transiently heats all plasma-viewing surfaces in order to desorb the tritium, which is released into the vessel and recovered by pumping. Calculations indicate significant tritium removal at reduced plasma current, ~6–10 MA, indicating the possibility of routine T recovery during the current rampdown phase of each discharge or during low current tritium recovery discharges.

© 2004 Elsevier B.V. All rights reserved.

PACS: 28.52.Fa; 52.40.Hf; 52.55.Fa; 28.52.Nh

Keywords: ITER; Tritium; Desorption; Hydrogen inventory; Ablation

1. Introduction

ITER is a proposed large tokamak whose mission is to study the physics of ‘burning plasmas’, i.e. a plasma whose temperature is primarily sustained by self-heating from deuterium–tritium (D–T) fusion in the plasma core [1]. Tritium is a radioactive hydrogenic (H) isotope that must be bred and recycled efficiently for D–T fusion energy production. Although ITER will not breed T, safety considerations will limit the ITER in-vessel inventory of T to 350 g. It is presently predicted that the T retention rate in ITER will be >3 g per 500 s pulse, primarily due to codeposition of T in redeposited carbon

(C) film layers formed by plasma erosion and deposition [2]. While carbon appears to be undesirable from the standpoint of T retention, transient heat loads to the wall from plasma disruptions and Edge Localized Modes make carbon-based plasma facing materials a necessity in the beginning phases of ITER, particularly in the divertor. In order to minimize the operational impact of T retention in ITER, and enhance device availability, it is necessary to develop routine, effective in situ techniques to recover T from the carbon deposits.

2. Description and calculations for H recovery

We use calculations, benchmarked to available experimental data, to examine the possibility of planned radiative plasma terminations (RPT) to recover tritium in ITER. The basic idea of the technique is to convert

* Corresponding author. Tel.: +1 608 262 4854; fax: +1 608 265 2364.

E-mail address: whyte@engr.wisc.edu (D.G. Whyte).

the high energy density of the ITER plasma into a nearly spatially uniform radiation pulse by massive impurity injection that benignly terminates the plasma discharge. The radiation pulse transiently heats all plasma-viewing surfaces in order to desorb the tritium, which is released into the vessel and recovered by pumping.

Heating plasma deposited carbon films to temperatures ≥ 1000 K recovers the tritium by enhancing H recombination and diffusion. Heating is the preferred recovery method for films on plasma-facing surfaces since the H is released predominately as diatomic H molecules [3], which can then be removed by the intrinsic vacuum pumping system. This is opposed to removing the films through oxidation [4] or ablation where the accompanying carbon from the eroded films must also be processed. However, only low temperatures bakes, $T_{\text{wall}} \sim 500$ K, are available for the water-cooled ITER wall, eliminating the possibility of recovering the T through steady-state bulk heating of the plasma-facing materials.

Transient surface heating of the films can be used for T recovery, since the T inventory resides primarily in surface films. Ex situ studies using radiative surface heating (with lasers and flashlamps [5,6]) of tokamak deposited films have measured efficient H/T recovery. A 1-D numerical model of the diffusive heat transfer and H release has been benchmarked against these studies (Fig. 1). The important feature is that the films have a reduced (but variable) thermal conductivity, $\kappa \sim 2$ W/m/K [7] and density $\rho \sim 1$ g/cm³, consistent with amorphous carbon and attains a high temperature compared to the substrate during the radiation pulse. The enhanced T_{surf} leads to substantial H release (using measured temperature dependent H diffusivity, Table 1) while the substrate material is relatively unaffected.

The RPT is initiated by a planned high-pressure noble gas injection demonstrated for disruption mitigation [8]. The KPRAD numerical model, which has been previously benchmarked for DIII-D and applied to ITER disruptions [9], is used to calculate the rapid evolution of the impurity ionization/radiation and the plasma energy balance for varying target plasma currents, I_p , in ITER (Figs. 2 and 3). The plasma stored thermal energy, W_{th} , is taken to decrease $\propto I_p^2$ (i.e. constant poloidal beta, β_p) with the assumption that auxiliary heating can replace the alpha heating lost for $I_p < 15$ MA where $W_{\text{th}} \sim 300$ MJ. A sufficient quantity of neon density is injected in ~ 5 ms to suppress conversion of the plasma current into relativistic runaway electrons in the ~ 100 ms current quench [8]. The plasma temperature collapses to $T_e \sim 3$ eV in about 1 ms due to intense impurity radiation (peak $q_{\text{rad}} \sim \text{GW m}^{-2}$, Fig. 3(b)), which is ideally isotropic to all plasma-viewing surfaces over ~ 680 m². The resulting surface temperature excursions for the bare, ‘substrate’ plasma-facing materials (carbon, beryllium, tungsten) do not surpass melt/abla-

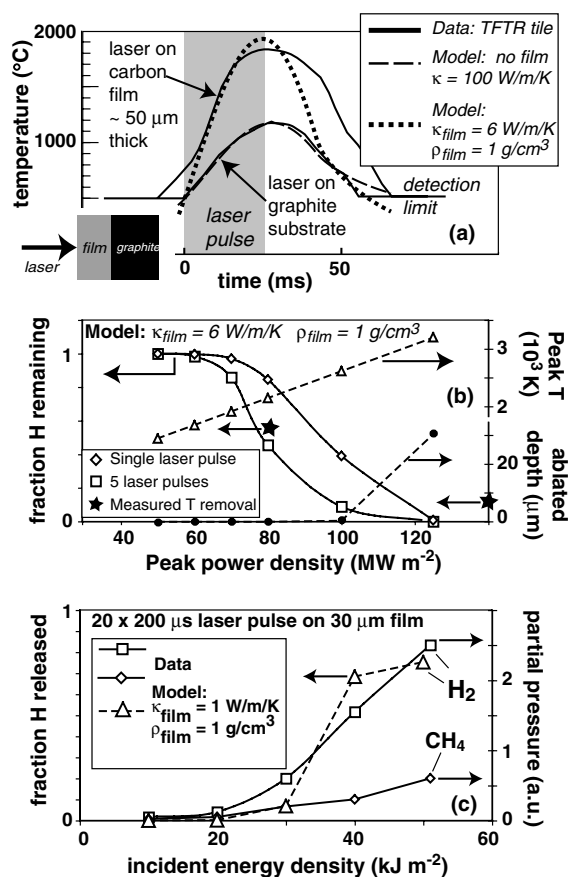


Fig. 1. Benchmarking of heat transfer and hydrogenic diffusion calculations for carbon deposition films. (a) Deposited films on TFTR graphite tiles have reduced κ and ρ , resulting in a higher temperature excursion than the substrate graphite ($\kappa = 100$ W/m/K, $\rho = 1.8$ g/cm³) for incident ~ 20 ms, 80 MW m^{-2} laser pulse [5]. (b) As above with varying incident laser power. For $T_{\text{surf}} > 2000$ K significant hydrogenic release occurs due to both single and multiple laser pulses. Carbon film ablation and total film H depletion occurs for $q \geq 120 \text{ MW m}^{-2}$ in the calculation. Measured tritium removal fractions (stars) [5] are compared. (c) Comparison of calculations with data from multiple ~ 0.2 ms laser pulses [6]. H₂ release becomes efficient after a threshold energy density $\sim 30 \text{ kJ m}^{-2}$. Measured H release is primarily in H₂ rather than the CH₄ hydrocarbon volatile.

tion limits with the exception of uniform Be melting for the $I_p = 15$ MA case.

After injection the neon atoms ionize, increasing plasma density and causing dilution cooling. The bulk of the plasma energy is then released by line radiation from low neon charge states ($Z \leq 3$) on a timescale of ~ 0.1 – 0.2 ms (Fig. 3(b)). This has two consequences. First, the plasma energy is dissipated by ‘soft’ radiation in the vacuum ultraviolet and visible range, $E_{\text{hv}} \leq T_e$, ensuring that radiation is deposited in a thin surface layer ($< 1 \mu\text{m}$). Secondly, there is a temporally non-uniform dissipation

Table 1

Parameters, A and B , for Arrhenius fitting of temperature dependent rates of interest. Rate $\equiv A \exp(-B/T)$ with temperature, T , in K

Rate	Units	A	B	Source
H diffusivity in film	$\text{m}^2 \text{s}^{-1}$	0.015	30 160	[3]
Carbon sublimation	m s^{-1}	84460	63 440	[7]
Carbon film erosion, 20 kPa O_2	m s^{-1}	6.9×10^{-5}	8850	[4]

Units of A as noted, B in K.

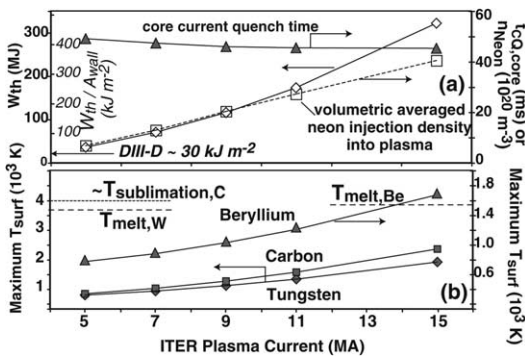


Fig. 2. Radiative termination for five different ITER target plasma currents, I_p . Open symbols: input parameters. Closed symbols: KPRAD [9] calculation results. (a) Plasma stored thermal energy, W_{th} , and energy density (W_{th}/A_{wall}) distributed over $A_{wall} \sim 680 \text{ m}^2$. Injected neon impurity density distributed through $V_{plasma} = 832 \text{ m}^3$ in 5 ms. Calculated core plasma L/R current quench time, $t_{CQ,core} \sim t_{CQ,net}/2.5$. (b) Maximum surface temperatures, T_{surf} , for ITER plasma-facing materials (without films).

of W_{th} that tends to increase the maximum surface temperature of the films.

The calculated q_{rad} is input to the heat/H diffusion model. An example calculation of depth-resolved carbon temperature and H release for the case of a 9 MA RPT on a 6 μm thick carbon film is shown in Fig. 3(c)–(d). In this case, peak $q_{rad} \sim 1 \text{ GW m}^{-2}$ and temperatures reaches ~ 2000 – 4000 K throughout the film, whilst the substrate temperature remains $< 1500 \text{ K}$. As expected for a temperature dependent diffusive process, the relative H release is much higher, $\sim 100\%$ in the first 4 μm , than for deeper in the film. With repetitive RPT application, this implies that there will be complete desorption in the near surface of subsequently deposited layers (Section 3). The overall H recovery efficiency from the film is $\sim 75\%$ and is expected to be primarily in the form of diatomic H molecules (DT, T₂, etc.). Based on T dependent C sublimation rates (Table 1), the surface temperature excursion to $T > 4000 \text{ K}$ results in ablation of $\sim 0.2 \mu\text{m}$ or $\sim 3\%$ of the film depth.

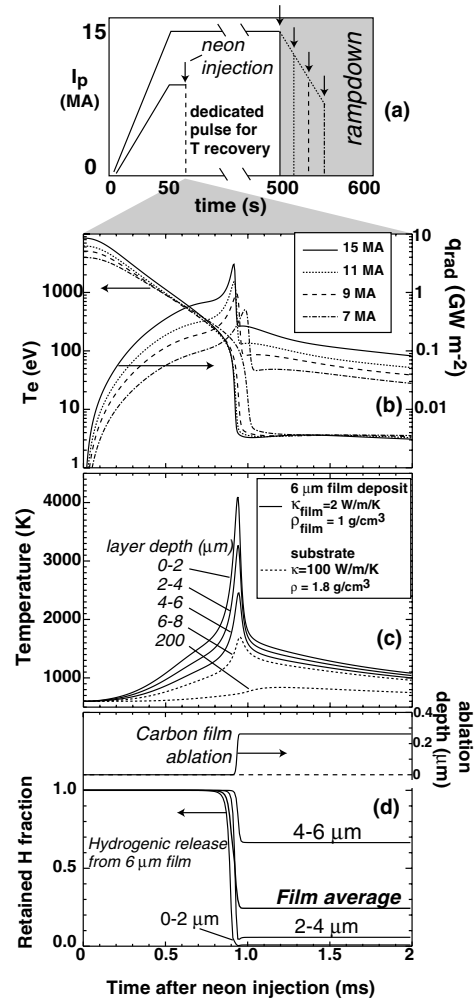


Fig. 3. (a) Radiative termination scenarios with varying plasma current: routine termination during I_p rampdown or dedicated short duration shots for T recovery. (b–d) Calculated time histories after neon injections. (b) Core averaged plasma electron temperature, T_e and radiative power density at plasma-viewing surfaces, q_{rad} for five I_p values. (c) Depth-resolved carbon temperatures through 6 μm film (with reduced thermal conductivity, κ , and density ρ) and the graphite substrate for target $I_p = 9 \text{ MA}$. (d) Depth-resolved and average H retention release from the 6 μm film in (c) and cumulative carbon film surface ablation.

Re-trapping of the released H in the films is limited since it is released into a cold plasma with shallow ion implantation ($\sim 10 \text{ nm}$). The absence of strong wall implantation is verified by present experiments: on DIII-D the injected impurity was absent in the the next discharge [9] and TFTR reported efficient ($\sim 10\%$) T inventory recovery by an unplanned 1.2 MA disruption [10].

A total release of 10 g of T into the ITER volume results in a modest H/D/T vessel pressure increase to ~50 Pa, similar to the partial pressure of the neon ~20 Pa. Therefore, after the plasma current has decayed in ~0.1 s the released D and T is recovered with high efficiency by the ITER cryopump (T inventory ~100 g) or roughing vacuum system [1].

3. Hydrogenic recovery from carbon films in ITER

Given the large number of variables regarding H desorption in a tokamak it is necessary that the scope of this present work be limited to providing a general validation of the recovery technique. We study neon RPT on carbon films by varying: target plasma $W_{th} \propto I_p^2$, $\kappa_{film} = 2\text{--}6\text{ W/m/K}$ (Fig. 1), and film depth 2–50 μm (a valid range since 100 m² of 10 μm saturated film (T/C ~ 0.2) \approx 50 g T inventory). Films with direct views of the plasma are considered, receiving q_{rad} as expected from the RPT calculation. This is appropriate for the majority of C films, which mostly grow on plasma-viewing surface in or near the divertor, due to line-of-sight deposition of high sticking fraction carbon [11]. Significant divertor radiative and conductive heating (~4–5% W_{th} , consistent with relative divertor volume) are found to occur with radiative terminations [9].

The results of this limited scoping study are presented in Figs. 4 and 5. Fig. 4 clearly shows that reduced I_p

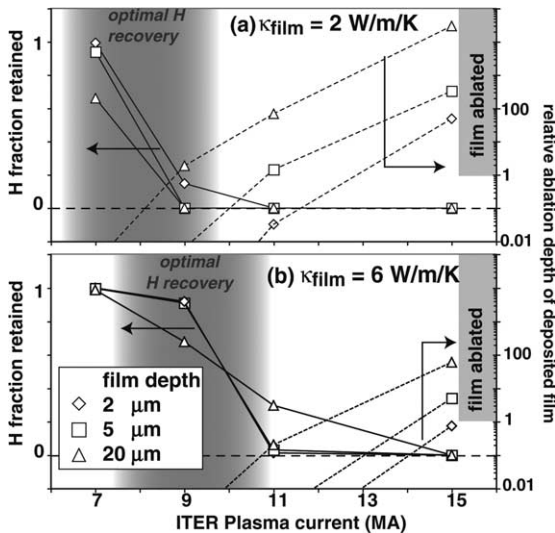


Fig. 4. Calculated H release (solid lines) and carbon ablation depth (dashed lines) for carbon films exposed to neon radiative termination at different plasma currents in ITER (Figs. 2 and 3). Results shown for three different film depth (or thickness). Results for films with thermal conductivity, $\kappa = 2\text{ W/m/K}$ (a) and $\kappa = 6\text{ W/m/K}$ (b) are shown. Lines are to guide the eye.

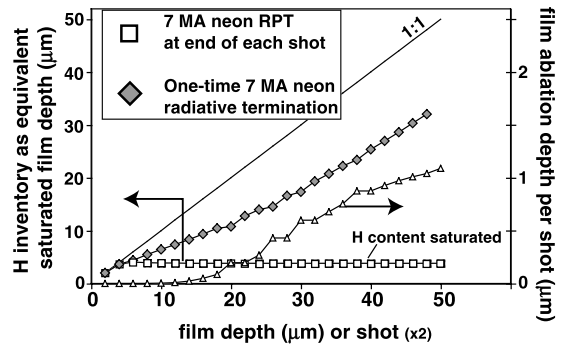


Fig. 5. Calculated H inventory (diamonds, squares) and carbon ablation depth (triangles) for carbon film with constant growth rate exposed to ITER neon RPT at $I_p = 7\text{ MA}$ (Figs. 2 and 3) for films with thermal conductivity, $\kappa = 2\text{ W/m/K}$. The 1:1 line shows continual H codeposited inventory buildup \propto film depth without radiative desorption. Diamonds: Reduced H inventory from a one-time RPT at the given film depth. Squares: Reduced (and saturated) H inventory when RPT is applied at the end of each shot.

(~6–10 MA) RPT's are favorable for T recovery. Substantial T recovery can occur without severely ablating the films. However the likely variability in tokamak film thickness and κ mean that there does not exist a single ideal I_p for T recovery. Fig. 5 indicates that an efficient means to limit T inventory in ITER is to apply low current (7 MA) RPT T recovery in the rampdown phase at the end of every discharge (Fig. 3(a)). As the film grows each shot, the peak T_{surf} caused by the repetitive RPT increases to the point where T is released from all but the deepest regions. This effectively saturates the buildup of T inventory in the film since subsequent deposition is on the film surface and is easily recovered. The effective saturation depth is ~2–20 μm depending on the film growth rate and κ_{film} , which may be acceptable for limiting the total ITER T inventory below 350 g.

20 kPa of O_2 injected ~0.15 s following a 9 MA neon RPT results in a peak erosion rate of 10 nm/s (Table 1), but a small cumulative erosion ~1 nm before the wall cools to <600 K. Therefore, oxygen (O_2) gas injection following the RPT is found to be ineffective at removing films, but thermal oxidation may still be required to remove soft films from non plasma-viewing surfaces.

4. Discussion and conclusions

The proposed RPT T recovery technique has several advantages. Tritium is possibly recovered from all plasma-viewing surfaces in a single event. No vessel entry is required. The T recovery is an integral part of plasma operations and T inventory is pro-actively minimized. The low- I_p termination greatly reduces collateral damage

to the vessel from halo current forces (poloidal field stored energy I_p^2), greatly reduces the threat of runaway electron conversion ($\propto e^{I_p}$ [12]), and eases technology demands for the RPT impurity delivery (gas jet, liquid jet, or pellet).

Figs. 4 and 5 indicate that some quantity of film ablation will result even from the use of low I_p RPT. This is not a fault per se of the RPT, but is a natural consequence of growing poor thermal conductivity films in a power intense environment, and eventually a balance between film growth and ablation will be established. The possible advantage of the RPT is that films will be highly T depleted when they eventually become mechanically unstable and fall off the substrate, creating mobile 'dust'. The RPT-induced film ablation will lead to 'plating' by line-of-sight coating or plasma deposition. Even though this occurs in a H rich environment, the ablation will likely form graphite-like, H depleted hard films due to the high local surface temperatures ($T > 1000$ K). Another concern is the effect of the ablation-caused film deposition on diagnostic viability. In this case a planned radiative termination is desired (as opposed to natural occurring ones from disruptions, etc.) since the long ITER pulse timescale (100's of second) allow for in situ protection to be implemented (shutters, isolation valves, etc.) before the RPT. Experience in present devices has indicated that the RPT itself is benign to plasma performance, and may even provide desired transient wall pumping for density control in the following discharge [9].

Our simple model of the RPT cannot capture the full complexity of T recovery in ITER. Fortunately there is significant operational flexibility in the controlling parameters, i.e. W_{th} (I_p , P_{aux}) and RPT frequency (in rampdown or dedicated recovery shots). Real-time operational decisions can be made balancing the plasma performance and device availability versus the ability to proactively control the T inventory. It is unlikely that by itself this technique will control T inventory in ITER,

but it could provide a powerful tool in reducing the frequency of more invasive recovery events, such as in-situ lasers [5] or O₂ baking [4].

We conclude that RPT appears promising as a flexible and proactive T recovery tool in ITER, and is complementary to invasive T recovery techniques presently being developed. Routine RPT, either during the ramp-down phase of each shot or during dedicated recovery shots, can saturate the T inventory buildup in films by continually depleting the near-surface codeposit layers.

Acknowledgments

We recognize G. Matthews for the initial research suggestion and C. Skinner for helpful comments. This work was supported by the US Department of energy under Grant No. DE-FG02-04ER54762 and by Natural Sciences and Engineering Research Council of Canada.

References

- [1] ITER Technical Basis, Report No. G A0 FDR 4 01-07-21 R 0.4, ITER (2001).
- [2] G. Federici et al., Nucl. Fusion 41 (2001) 1967.
- [3] J. Winter et al., Nucl. Instrum. and Meth. B 23 (1987) 538.
- [4] J.W. Davis et al., J. Nucl. Mater. 266–269 (1999) 478.
- [5] C.H. Skinner et al., Report No. PPPL-3630rev, Princeton Plasma Physics Laboratory (2001).
- [6] K.J. Gibson et al., IEA Workshop on In-vessel Tritium Inventory, Culham Science Centre, Abingdon, UK, 2003.
- [7] CRC Handbook of Chemistry & Physics 65, CRC, 1984.
- [8] D.G. Whyte et al., Phys. Rev. Lett. 89 (2002) 055001.
- [9] D.G. Whyte et al., J. Nucl. Mater. 313–316 (2003) 1239.
- [10] C.H. Skinner et al., J. Vac. Sci. Technol. A 14 (1996) 3267.
- [11] M. Mayer et al., Phys. Scr. T 111, in press.
- [12] M.N. Rosenbluth et al., Nucl. Fusion 37 (1997) 1355.